Limitations on the Size of Miniature Electric-Field Probes

GLENN S. SMITH, SENIOR MEMBER, IEEE

Abstract—**The miniature dipole probe is a useful tool for measuring the electric field at high radio and microwave frequencies. A common design for the probe consists of an electrically-short antenna with a diode across its terminals; a resistive, parallel-wire transmission line transmits the detected signal from the diode to the monitoring instrumentation. Small dipoles are desirable because they provide high spatial resolution of the field, and because they permit a frequency-independent response at higher microwave frequencies. Recent efforts have produced probes with dipole half lengths h less than one millimeter. With the advances occuring in microelectronics and thin-film technology, the construction of even smaller probes may be possible.**

In this paper, the limitations imposed on the sensitivity of the probe by a reduction in its physical size are determined. A model that contains noise sources for the diode and the resistive transmission line is used to obtain the signal-to-noise ratio for the probe, and this is examined as a function of the parameters that describe the dipole, diode, resistive transmission line, and amplifier. When the physical dimensions of the probe are reduced by the scale factor k_l ($k_l < 1$), the signal-to-noise ratio is found to decrease by approximately the factor k_l^4, and the minimum-detectable incident electric field for a fixed signal-to-noise ratio is found to increase by approximately the factor k_l^{-2}. A numerical estimate is made for the sensitivity of miniature probes with dipole half lengths in the range 10 μm $\leq h \leq$ 1 cm.

I. Introduction

A DIPOLE ANTENNA that is electrically and physically small is a useful probe for measuring electric fields of unknown strength. The current interest in the biological applications and the possible health hazards of nonionizing electromagnetic radiation has led to the development of miniature dipole probes for use in monitoring fields both in free space and in material media. The physical size of the miniature field probe has been continuously reduced. Operational probes with dipole half lengths h less than 0.8 mm have been developed by the U.S. Bureau of Radiological Health and by its contractors [1]–[3], and experimental probes with h as small as 0.3 mm have been produced at the University of Virginia, Charlottesville [4]. With the advances occuring in microelectronics and thin-film technology, the construction of even smaller probes may be possible. The subject of this paper is the limitations imposed on the response of these probes by a decrease in their physical size.

A schematic drawing of a typical dipole receiving probe is shown in Fig. 1. The operation of this probe is fairly simple. For an amplitude-modulated incident field, the dipole produces an amplitude-modulated oscillating voltage across the diode at its terminals. When the diode is operating in its square-law region, a current proportional to the square of the modulating signal is also developed at the diode. For example, a continuous-wave field produces a direct current at the diode. This current is passed through the low-pass filter formed by the lossy transmission line to the monitoring amplifier. Thus, a signal proportional to the square of the amplitude modulation on the incident field is measured. The high-resistance per-unit-length of the lossy transmission line reduces the signal received directly by the line and transmitted to the diode; it also reduces the scattering of the incident field by the transmission line. A transmission line formed from two different sections is shown in Fig. 1; the section nearest the dipole, line 1, has the highest resistance per unit length.

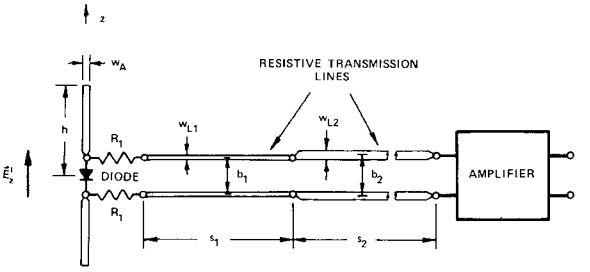

Fig. 1. Model for dipole receiving probe.

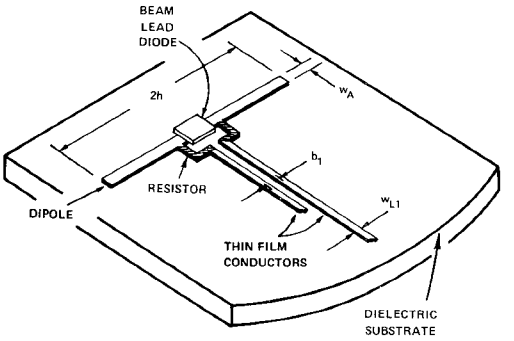

Fig. 2. Detail of typical construction for miniature electric-field probes.

Fig. 2 shows a typical construction for the miniature electric-field probe. The conductors of the resistive transmission lines and the discrete resistors are formed by depositing thin metallic films on a dielectric substrate. The diode is usually an unbiased Schottky barrier diode of

Manuscript received August 24, 1983; revised February 2, 1984. This work was supported in part by the National Science Foundation under Grant ECS-8105163 and by the Joint Services Electronics Program under Contract DAAG29-81-K-0024.

The author is with the School of Electrical Engineering, Georgia Institute of Technology, Atlanta, GA 30332.

0018-9480/84/0600-0594$01.00 ©1984 IEEE

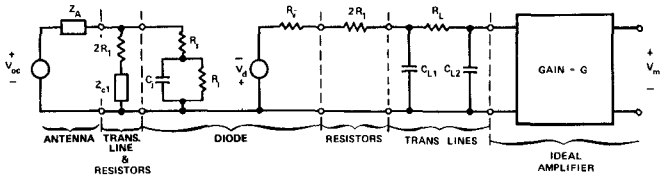

Fig. 3. Equivalent circuit for probe.

beam-lead construction with the leads forming all or part of the dipole antenna.

II. Detected Signal

In the model for the miniature probe shown in Fig. 1, the dipole and the conductors of the two transmission lines are formed from flat strips with the widths w_A, w_{L1}, and w_{L2}, respectively. The half length of the dipole is h, and the lengths and spacings of the transmission line conductors are s_1, s_2 and b_1, b_2. The resistivities and thicknesses of the thin films forming the conductors of the transmission lines are adjusted to produce the resistances per unit length r_1^i and r_2^i.[1] The capacitances per unit length of the lines are c_1 and c_2.

The response of the miniature probe is easily determined from the equivalent circuit shown in Fig. 3. Detailed discussions of this circuit are given in [5, ch. 3] and in [6]; the analysis of the circuit will only be summarized here.

In the high-frequency portion of the equivalent circuit, the dipole antenna is represented by its Thévenin equivalent. The open-circuit voltage at the terminals of the electrically-short receiving dipole is approximately proportional to the component of the incident electric field parallel to the axis of the dipole (z axis)

$$V_{0c} \approx hE_z^i \tag{1}$$

and the input impedance of the electrically-short dipole is approximately capacitive[2]

$$Z_A \approx -j/\omega C_A \tag{2a}$$

where

$$C_A \approx \pi\epsilon_0\epsilon_{er}h/[\ln(4h/w_A)-1]. \tag{2b}$$

The effective relative permittivity ϵ_{er} is included in (2b) to account for the dipole being on a dielectric substrate.

The high-frequency circuit for the diode is the junction impedance R_j in parallel with C_j, in series with the resistor R_s. The resistor R_s is small (typically $R_s = 5$ to 25 Ω), and will be omitted in the following analysis where it is assumed that $R_j \gg R_s$ and $\omega C_j R_s \ll 1$.

The complex wave number for the highly-resistive transmission line, line 1, is approximately $k_{L1} \approx \sqrt{\omega r_1^i c_1}(1-j)$. The parameters, viz, r_1^i, c_1, and s_1, of this line are chosen so that the transfer function τ for a wave propagating over the line is small at the frequencies of interest, i.e.

$$\tau = |e^{-jk_{L1}s_1}| \ll 1. \tag{3a}$$

The input impedance to transmission line 1 is then approximately its characteristic impedance Z_{c1} [7]

$$Z_{c1} = R_{c1} + jX_{c1} \approx \sqrt{r_1^i/\omega c_1}(1-j). \tag{3b}$$

This impedance in series with the resistance $2R_1$ appears across the diode. The discrete resistors R_1 are included to keep the transmission line from presenting a low impedance across the diode at high frequencies.

In the low-frequency portion of the equivalent circuit, the diode is modeled by the voltage source V_d in series with the video resistance R_v

$$V_d \approx \gamma_0 P \tag{4a}$$

where γ_0 is the voltage sensitivity and P is the time average of the high-frequency power absorbed by the junction resistance R_j of the diode. Note that γ_0 is the voltage sensitivity of the diode junction; it is not to be confused with the voltage sensitivity after compensation for the effects of junction capacitance, load resistance, and reflection loss [8]. The latter is sometimes reported in manufacturers' specifications. The current sensitivity is

$$\beta_0 = \gamma_0/R_v. \tag{4b}$$

For an ideal diode at a temperature of 290 K, $\beta_0 \approx 20$ A/W.

The low-frequency model for the two resistive transmission lines in series is the "Pi" equivalent network with the elements

$$R_L = 2(r_1^i s_1 + r_2^i s_2) \tag{5a}$$

$$C_{L1} = \frac{c_1 s_1}{2}\left[1 + \frac{r_2^i s_2(c_1 s_1 + c_2 s_2)}{c_1 s_1(r_1^i s_1 + r_2^i s_2)}\right] \tag{5b}$$

$$C_{L2} = \frac{c_2 s_2}{2}\left[1 + \frac{r_1^i s_1(c_1 s_1 + c_2 s_2)}{c_2 s_2(r_1^i s_1 + r_2^i s_2)}\right]. \tag{5c}$$

This network is obtained by combining two "Pi" networks, one representing each of the transmission lines, and dropping terms of order $\omega r_1^i s_1 r_2^i s_2(c_1 s_1 + c_2 s_2)/(r_1^i s_1 + r_2^i s_2)$. When a single resistive transmission line is used, the elements in the network are

$$R_L = 2r's, \qquad C_{L1} = C_{L2} = cs/2. \tag{6}$$

Note that the "Pi" network is a low-pass filter. When it is driven by an ideal voltage source and terminated in an open circuit, the 3-dB cutoff frequency is

$$\omega_L = 2\pi f_L = (R_L C_{L2})^{-1} = [r_1^i s_1(c_1 s_1 + 2c_2 s_2) + r_2^i s_2 c_2 s_2]^{-1}. \tag{7}$$

The low-frequency amplifier is assumed to be an ideal noiseless amplifier with gain G, a "brickwall" passband of bandwidth $\Delta\omega = 2\pi\Delta f$, and an infinite input impedance.[3]

[1] The thicknesses of the thin films are assumed to be small compared with the skin depths in the resistive materials at the frequencies of interest, so that the resistances per unit length r^i are approximately frequency independent.

[2] Here the thin strip of width w_A is assumed to be approximately equivalent to a circular conductor of radius $a = w_A/4$.

[3] The capacitance at the input to the amplifier can be included in the analysis by simply adding it to the capacitor C_{L2}.

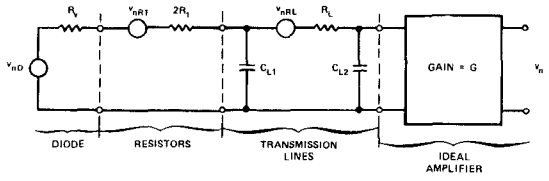

Fig. 4. Noise equivalent circuit for probe.

The assumption of an ideal amplifier simplifies the analysis and permits a discussion of the probe's characteristics, such as its signal-to-noise ratio, independent of the particular amplifier used.

For a continuous-wave incident field (unmodulated signal), the detected signal $|V_m|$ at the terminals of the amplifier, as determined from the equivalent circuit in Fig. 3, is

$$|V_m| = \frac{G(\omega R_j C_A)^2 \gamma_0 |V_{0c}|^2}{2R_j\left\{\left[1+R_j(2R_1+R_{c1})/|2R_1+Z_{c1}|^2\right]^2+\left[\omega/\omega_c - R_j X_{c1}/|2R_1+Z_{c1}|^2\right]^2\right\}} \tag{8}$$

with

$$\omega_c = \left[R_j(C_A+C_j)\right]^{-1}. \tag{9}$$

III. Noise Analysis

The noise voltage at the terminals of the amplifier is obtained from the noise equivalent circuit shown in Fig. 4. Each of the noise-voltage sources $v_n(t)$ in the circuit is associated with a time-average, one-sided, (voltage) power-density spectrum $P_n(f)$. The noise power-density spectra for the two thermal-noise sources, the resistances $2R_1$ and R_L, are

$$P_{nR1}(f) = 4kT(2R_1) \tag{10}$$

$$P_{nRL}(f) = 4kTR_L \tag{11}$$

where Boltzmann's constant $k = 1.38\times10^{-23}$ J/K, and T is the temperature in degrees Kelvin [9], [10].

The noise power-density spectrum for the diode is approximately [11]–[13]

$$P_{nD}(f) = 4kTR_v t_w(1+f_N/f_V) \tag{12}$$

where t_w is the "white noise temperature ratio," f_V the video frequency, and the term f_N/f_V accounts for the "$1/f$ noise" or "flicker noise" of the diode. The diode in the miniature probe is essentially unbiased. No external bias is applied to the diode, and the self bias is very small due to the large series resistance in the low-frequency circuit. For an unbiased diode, $t_w \approx 1$ and $f_N \approx 0$; therefore, the noise power-density spectrum of the diode is approximately

$$P_{nD}(f) \approx 4kTR_v. \tag{13}$$

The mean-squared noise voltage at the output of the amplifier is

$$\langle v_n^2\rangle = G^2\left[(P_{nR1}+P_{nD})\int_0^{\Delta f}|H_D(f)|^2\,df + P_{nRL}\int_0^{\Delta f}|H_L(f)|^2\,df\right] \tag{14}$$

where the fact that the spectra of the three noise sources (10), (11), and (13) are approximately frequency independent has been used. The squares of the magnitudes of the voltage transfer functions $H_D(\omega)$ and $H_L(\omega)$ are

$$|H_D(\omega)|^2 = \left[\left(\omega^2/\omega_L\omega_R\right)^2+\left(\omega^2/\omega_L\omega_R\right)\ell+1\right]^{-1} \tag{15}$$

$$|H_L(\omega)|^2 = \left[1+(\omega/\omega_R)^2\right]/\left[\left(\omega^2/\omega_L\omega_R\right)^2 + \left(\omega^2/\omega_L\omega_R\right)\ell+1\right] \tag{16}$$

with

$$\omega_R = \left[(R_v+2R_1)C_{L1}\right]^{-1} \tag{17}$$

and

$$\ell = (\omega_L/\omega_R)(1+C_{L2}/C_{L1})^2+\omega_R/\omega_L+2C_{L2}/C_{L1}. \tag{18}$$

The integrals in (14) can be evaluated in closed form [14]; after considerable reduction, one obtains the root-mean-square (RMS) noise voltage at the output of the amplifier

$$\langle v_n^2\rangle^{1/2} = G\left[\frac{2kT\sqrt{\omega_L\omega_R}}{\pi h}\cdot\left(\frac{1}{\sqrt{f}}\tan^{-1}\left(\Delta\omega/\sqrt{\omega_L\omega_R f}\right)\cdot\left\{2R_1+R_v + R_L\left[1-(\omega_L/\omega_R)f\right]\right\} - \frac{1}{\sqrt{g}}\tan^{-1}\left(\Delta\omega/\sqrt{\omega_L\omega_R g}\right)\cdot\left\{2R_1+R_v+R_L\left[1-(\omega_L/\omega_R)g\right]\right\}\right)\right]^{1/2} \tag{19}$$

where

$$h = \sqrt{\ell^2-4} \tag{20a}$$

$$f = (\ell-h)/2 \tag{20b}$$

$$g = (\ell+h)/2 \tag{20c}$$

and it is assumed that $h^2 > 0$.

TABLE I
PARAMETERS FOR BRH PROBE.

Antenna	Transmission Lines	
$h = 0.75$ mm	$s_1 = 3.0$ cm	$s_2 = 24.7$ cm
$w_A = 0.20$ mm	$b_1 = 100\ \mu$m	$b_2 = 1.5$ mm
Diode	$w_{L1} = 50\ \mu$m	$w_{L2} = 0.75$ mm
	$r'_1 = 5$ MΩ/m	$r'_2 = 333$ kΩ/m
$R_j = R_v = 400$ kΩ	$c_1 = 30$ pF/m	$c_2 = 30$ pF/m
$C_j = 0.1$ pF	$2R_1 = 2.5$ KΩ	
$\beta_0 = 20$ A/W	ε_{er} (substrate) = 2.0	

IV. Signal-to-Noise Ratio

With the expressions for the detected signal (8) and the RMS noise voltage (19) available, the signal-to-noise (S/N) at the output of the amplifier is determined

$$S/N = |V_m|/\langle v_n^2\rangle^{1/2}. \tag{21}$$

This expression is easily inverted to find the minimum incident electric field $|E_z^i|$ that can be detected for a given signal-to-noise ratio.

To test the theory, a numerical calculation was made for a miniature probe for which experimental data are available. The probe considered was developed by the U.S. Bureau of Radiological Health and the Narda Microwave Corporation (BRH Model 10, Narda Model 25256); it has a dipole half length $h = 0.75$ mm; approximate values for the other parameters that describe the probe are listed in Table I.

In measurements made by the Bureau of Radiological Health, a signal-to-noise ratio of 10 for a 1-Hz detector bandwidth ($\Delta f = 1$ Hz) was obtained with this probe in an incident plane-wave field at the frequency $f = 2.45$ GHz and at a power density of 0.05 mW/cm^2 (peak incident electric field $|E_z^i| = 19.4$ V/m) [3]. A similar probe (Narda Model 2608) was tested at the University of Ottawa; their measurements at the frequency $f = 1.0$ GHz show that a peak incident electric field $|E_z^i| = 7.7$ V/m is required for the same signal-to-noise ratio and detector bandwidth [15]. A theoretical calculation made by using (8), (19), and (21) indicates that an incident electric field $|E_z^i| = 2.5$ V/m can be detected under the same conditions. The agreement between the measured and the calculated incident fields (they differ by factors of 7.8 and 3.1) is surprisingly good, considering that the parameters for the diode are only typical values for the type of diode used and that no account was taken of the noise in the amplifiers.

V. Sensitivity Versus Probe Size

One objective of this study is to determine the signal-to-noise ratio and the minimum incident electric field $|E_z^i|$ that can be detected for a given signal-to-noise ratio as the physical size of the probe is decreased. The expressions (8) and (19) for the detected signal and the noise voltage are too complex in their present form to extract any general dependence of the sensitivity on the parameters that describe the probe. The complexity of these expressions, however, can be greatly reduced by making a few simple assumptions.

The impedance $2R_1 + Z_{c1}$ that shunts the diode in the high-frequency equivalent circuit, Fig. 3, is chosen to be large compared with the diode impedance, i.e., $|2R_1 + Z_{c1}| \gg R_j$. This prevents the impedance from "loading down" the diode. In addition, the junction resistance and the video resistance of the diode are taken to be approximately equal, $R_v \approx R_j$. The voltage sensitivity of the diode γ_0 can be expressed in terms of the current sensitivity (4b), $\gamma_0 = \beta_0 R_v \approx \beta_0 R_j$. With these assumptions, the detected signal (8) becomes

$$|V_m| \approx G\beta_0 \left(\frac{C_A}{C_A + C_j}\right)^2 \frac{h^2 |E_z^i|^2}{2} \left(\frac{1}{1 + \omega_c^2/\omega^2}\right). \tag{22}$$

If $\omega^2 \gg \omega_c^2$, the response of the probe is independent of frequency, and (22) is simplified

$$|V_m| \approx G\beta_0 \left(\frac{C_A}{C_A + C_j}\right)^2 \frac{h^2 |E_z^i|^2}{2}. \tag{23}$$

The total resistance of the transmission lines $R_L = 2(r_1^i s_1 + r_2^i s_2)$ is chosen to be much greater than the resistance $2R_1 + R_v$, i.e., $R_L \gg 2R_1 + R_v$, making $\omega_L/\omega_R \ll 1$ for C_{L1} and C_{L2} of comparable value. With this assumption, the noise voltage (19) becomes

$$\langle v_n^2\rangle^{1/2} \approx G\sqrt{\frac{2kT}{\pi C_{L2}} \tan^{-1}(\Delta\omega/\omega_L)}. \tag{24}$$

Simplified approximate expressions for the signal-to-noise ratio and the minimum-detectable incident electric field for a fixed S/N result from the use of (23) and (24) in (21)

$$S/N \approx \frac{\beta_0 h^2 |E_z^i|^2 \left[C_A/(C_A + C_j)\right]^2}{2\sqrt{\frac{2kT}{\pi C_{L2}} \tan^{-1}(\Delta\omega/\omega_L)}} \tag{25}$$

$$|E_z^i| \approx \left[2(S/N)\sqrt{\frac{2kT}{\pi C_{L2}} \tan^{-1}(\Delta\omega/\omega_L)}\ /\beta_0 h^2\right]^{1/2} \cdot (1 + C_j/C_A). \tag{26}$$

Note that the inequalities used in obtaining (22) and (24), $|2R_1 + Z_{c1}| \gg R_j$ and $R_L \gg 2R_1 + R_v$, can be satisfied by choosing a diode with a suitably low junction or video resistance, since $2R_1$ is of the order of R_j or R_v. These inequalities, however, are not the only conditions that must be considered when choosing R_j. The junction resistance also enters the expression for the frequency ω_c (9) which is the lower bound for the frequency-independent response of the probe. A discussion of this phenomenon is in [6].

It is interesting to examine the expression for the noise voltage (24) for two limiting cases, i) the bandwidth of the amplifier equal to the 3-dB cutoff frequency of the transmission lines, $\Delta\omega/\omega_L = 1$, and ii) the bandwidth of the amplifier much less than the 3-dB cutoff frequency of the transmission lines, $\Delta\omega/\omega_L \ll 1$. In the first case, (24) becomes

$$\langle v_n^2\rangle^{1/2} \approx G\sqrt{\frac{kT}{2C_{L2}}}. \tag{27}$$

When the resistance of the first transmission line is much greater than that of the second ($r_1^i s_1 / r_2^i / s_2 \gg 1$), the capacitance C_{L2} (5c) and the noise voltage (27) are nearly independent of the resistance of the transmission lines R_L. This is the result of the noise power-density spectrum P_{nRL} of the transmission lines being proportional to R_L and the bandwidth of the amplifier $\Delta\omega$ being proportional to R_L^{-1}, which makes the product $R_L \Delta\omega$ independent of R_L. In the second case, (24) becomes

$$\langle v_n^2 \rangle^{1/2} \approx G\sqrt{4kTR_L \Delta f}. \tag{28}$$

This is just the noise voltage produced by the resistance of the transmission lines R_L in the bandwidth $\Delta f = \Delta\omega/2\pi$. In both of these cases, the expression for the minimum-detectable electric field for a fixed S/N (26) involves c_j and only two parameters that describe the probe: the half length of the dipole h, and the transmission-line capacitance C_{L2} (case i) or the transmission-line resistance R_L (case ii). Of these parameters, a variation in h has the greatest effect on $|E_z^i|$, since it enters the expression as h^{-1} when $C_j \ll C_A$ or as h^{-2} when $C_j \gg C_A$, whereas the other parameters enter the expression as $C_{L2}^{-1/4}$ and $R_L^{1/4}$.

The highly resistive transmission line, line 1, must be designed to not interfere with the reception of the incident field by the dipole antenna.[4] This is accomplished by making the transfer function for a wave propagating over the line

$$\tau = \exp\left(-\sqrt{\omega r_1^i c_1}\, s_1\right) \tag{29}$$

small, as in (3a), and by making the reception of the incident field by the transmission line negligible. The ratio of the signal received by the transmission line to the signal received by the dipole is proportional to

$$\chi |Z_{c1}/(Z_{c1} + 2R_1)| \tag{30a}$$

with

$$\chi = \frac{[\ln(4h/w_A) - 1]}{\pi}(b_1/h)(\zeta_0/2r_1^i h) \tag{30b}$$

and ζ_0 equal to the impedance of free space [7]. The reception by the transmission line is negligible when the dimensionless parameter χ is small, i.e., $\chi \ll 1$. With τ and χ specified, (29) and (30b) can be rewritten to obtain expressions for the resistance per-unit-length r_1^i and the length s_1 of line 1

$$r_1^i = \zeta_0(b_1/h)[\ln(4h/w_A) - 1]/2\pi h\chi \tag{31}$$

$$s_1 = -\ln(\tau)/\sqrt{\omega r_1^i c_1}. \tag{32}$$

Now consider a reduction in the size of the probe that leaves the performance of the highly-resistive transmission line approximately unchanged, i.e., the parameters τ (29) and χ (30b) unchanged. The dimensions of the dipole (h and w_A) are reduced by the scale factor k_l ($k_l < 1$). The widths and the spacings of the conductors for both transmission lines (w_{L1}, w_{L2} and b_1, b_2) are also reduced by the same scale factor. The capacitances per-unit-length for both of the transmission lines c_1 and c_2 are then nearly independent of k_l.[5]

The remaining parameters for line 1, r_1^i and s_1, are determined from (31) and (32) once the constants τ and χ are specified. Note that the resistance per unit length r_1^i must be increased as k_l^{-1} and the length s_1 decreased as $k_l^{1/2}$. The scaling for r_1^i can be accomplished by holding fixed the thickness t_{L1} of the resistive film forming the conductors of the line as the size of the probe is reduced ($r_1^i \propto 1/w_{L1}t_{L1}, w_{L1} \propto k_l$).

The length of line 2 is held fixed, since it determines the spacing between the dipole and the instrumentation, and the resistance of line 2 is assumed to be much smaller than the resistance of line 1, $r_2^i s_2 \ll r_1^i s_1$. This makes the capacitors C_{L1} and C_{L2}, (5b) and (5c), and the cutoff frequency ω_L (7) in the equivalent circuit for the transmission lines nearly independent of $r_2^i s_2$:

$$C_{L1} \approx c_1 s_1/2$$

$$C_{L2} \approx c_1 s_1/2 + c_2 s_2$$

$$\omega_L \approx \left[r_1^i s_1 (c_1 s_1 + 2c_2 s_2)\right]^{-1}.$$

With the scaling described above, the dependence of the signal-to-noise ratio (25) on the scale factor k_l is easily determined. Usually, $C_j \gg C_A$ for very short dipoles, making the numerator of (25) approximately proportional to h^4 or k_l^4. The denominator of (25) is only weakly dependent on k_l; for example, when $\Delta\omega \ll \omega_L$ the denominator is proportional to $k_l^{-1/4}$. Thus, the signal-to-noise ratio is seen to decrease approximately as k_l^4. The same argument shows that the minimum-detectable incident electric field $|E_z^i|$ for a fixed S/N (26) increases as k_l^{-2}.

In Fig. 5, the minimum-detectable incident electric field $|E_z^i|$, obtained from (26), for a signal-to-noise ratio of 10 dB ($S/N = 3.16\ldots$) is shown as a function of the half length of the dipole. The scaling described above was used in preparing this graph. The parameters chosen for the dipole and the transmission lines are $h/w_A = 5.0$, $\epsilon_{er} = 1.0$, $b_1/h = 0.2$, $c_2 s_2 = 10$ pF; those for the diode are $C_j = 0.1$ pF, and $\beta_0 = 20.0$ A/W (the theoretical value for an ideal diode), and the temperature is 290 K. In addition, the dimensionless parameters τ (29) and χ (30b) are assumed to be $\tau = 0.01$ at the frequency $f = 100$ MHz and $\chi = 0.01$. Results are shown for the bandwidth of the amplifier equal to 1 Hz and equal to the 3-dB cutoff frequency of the transmission lines. Curves are presented for typical values of the capacitance per unit length of transmission line 1,

[4]The transmission line must also be designed so that the amount of energy it scatters is acceptable for a particular application. Formulas for the scattering cross section of the line are in [7].

[5]The thicknesses of the thin-film conductors are assumed small compared with their widths, and the thickness of the dielectric substrate is assumed large compared with the dimensions of the transmission-line cross sections.

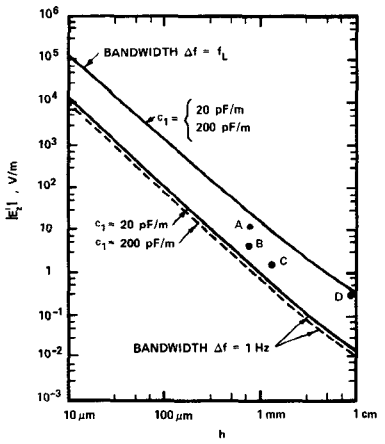

Fig. 5. The minimum-detectable peak electric field $|E_z^i|$ for a 10-dB signal-to-noise ratio versus the dipole half length h. The parameters for the theoretical calculations are given in the text. The measured data are for: a) BRH Model 10, Bassen and Franke [3], $f = 2.45$ GHz; b) Narda Model 2608, Stuchly, *et al.* [15], $f = 1.0$ GHz; c) EIT Model 979, Stuchly, *et al.* [15], $f = 1.0$ GHz; d) Holaday Model IME-01, Stuchly, *et al.* [15], $f = 1.0$ GHz.

$c_1 = 20$ pF/m and 200 pF/m. The parameters used in Fig. 5 for the transmission lines are only typical values; changes in these parameters will affect the calculated values for $|E_z^i|$. However, the variation in $|E_z^i|$ with these parameters will be fairly slow, since they enter the expression for $|E_z^i|$ (26) as arguments of a fourth root.

From Fig. 5, it is clear that the price paid for a decrease in the size of the miniature field probe is a drastic decrease in the sensitivity. Even for a 1-Hz detection bandwidth and only a 10-dB signal-to-noise ratio, the half length of the dipole must be greater than about 1 mm to measure a peak electric field of 1 V/m. With the detection bandwidth equal to the 3-dB cutoff frequency of the transmission lines, the half length of the dipole would have to be greater than about 0.5 cm to measure the same electric field.

Of course, a decrease in the length of the dipole has the advantageous effect of increasing the maximum electric field that can be measured with the probe, i.e., a larger electric field can be measured before the voltage across the junction of the diode is sufficient to cause a departure from square-law response. However, there are other preferred methods for correcting for non-square-law response that do not affect the sensitivity of the probe, such as the use of shaping circuitry in the monitoring instrumentation [16].

The measured results of other investigators for probes with half lengths in the range $0.75 \text{ mm} \leqslant h \leqslant 8.9$ mm are also shown in Fig. 5 [3], [15]. In all cases, the measured data have been converted to give the minimum-detectable, peak electric field for a 10-dB signal-to-noise ratio with a 1-Hz bandwidth. The measured points are seen to follow the trend of the theoretical estimate, but they are higher by factors of three to twenty. This is to be expected, since some of the parameters for these probes are quite different from those used in the theoretical calculations. The theoretical curves can be considered as reasonable estimates of the sensitivity to be expected from miniature electric-field probes of the design shown in Fig. 1 and with the specified values of τ and χ.

Currently, the beam-lead diodes available commercially have a junction size of the order of 100 μm. Probes constructed using these diodes, even with some modification to the diode, are limited to dipole half lengths greater than about $h = 0.3$ mm [4]. New diodes would have to be fabricated before probes with smaller dipoles could be constructed.

VI. Conclusion

The miniature electric-field probe with the construction shown in Fig. 1 was analyzed to determine its signal-to-noise ratio and the minimum-detectable incident electric field for a fixed signal-to-noise ratio. A method for scaling the physical dimensions of the elements in the probe was presented, and the variation in the sensitivity of the probe with a decrease in its physical size by the factor k_l ($k_l < 1$) was examined. The signal-to-noise ratio for the probe was found to decrease approximately as k_l^4, and the minimum-detectable incident electric field for a fixed signal-to-noise ratio was found to increase approximately as k_l^{-2}. The formulas and numerical results presented should be helpful in the design of future miniature electric-field probes.

Acknowledgment

The author wishes to thank H. Bassen and K. Franke of the Bureau of Radiological Health for supplying the data for the BRH electric field probe, and Prof. M. Stuchly of the University of Ottawa for permission to use her measured data prior to publication. The author also wishes to thank T. Batchman of the University of Virginia for several helpful discussions on the fabrication of miniature field probes and J. Nordgard for a critical reading of the manuscript.

References

[1] H. Bassen, M. Swicord, and J. Abita, "A miniature broad-band electric field probe," *Annals New York Academy Sciences*, Biological Effects of Nonionizing Radiation, vol. 247, pp. 481–493, Feb. 1975.

[2] H. Bassen, W. Herman, and R. Hoss, "EM probe with fiber optic telemetry," *Microwave J.*, vol. 20, pp. 35–39, Apr. 1977.

[3] H. Bassen and K. Franke, "BRH implantable probe evaluation-October 1978," Unpublished Report, Bureau of Radiological Health, Rockville, MD, Oct. 1978.

[4] T. E. Batchman and G. Gimpleson, "An implantable electric-field probe of subminiature dimensions," *IEEE Trans. Microwave Theory Tech.*, vol. MTT-31, pp. 745–751, Sept. 1983.

[5] R. W. P. King and G. S. Smith, *Antennas in Matter: Fundamentals, Theory and Applications*. Cambridge, MA: M.I.T. Press, 1981, ch. 3.

[6] H. I. Bassen and G. S. Smith, "Electric field probes–A review," *IEEE Trans. Antennas Propagat.*, vol. AP-31, pp. 710–718, Sept. 1983.

[7] G. S. Smith, "Analysis of miniature electric field probes with resistive transmission lines," *IEEE Trans. Microwave Theory Tech.*, vol. MTT-29, pp. 1213–1224, Nov. 1981.

[8] J. Lepoff, "How the new Schottkys detect without DC bias," *Microwaves*, vol. 16, pp. 44–48, Feb. 1977.

[9] F. N. H. Robinson, *Noise and Fluctuations in Electronic Devices and Circuits*. London: Oxford University Press, 1974.

[10] M. Javid and E. Brenner, *Analysis, Transmission and Filtering of Signals*. New York: McGraw-Hill, 1963, ch. 9.

[11] G. R. Nicoll, "Noise in silicon microwave diodes," *Proc. Inst. Elec. Eng.*, part 3, vol. 101, pp. 317–324, Sept. 1954.
[12] A. Uhlir, Jr., "Characterization of crystal diodes for low-level microwave detection," *Microwave J.*, vol. 6, pp. 59–67, July 1963.
[13] A. M. Cowley and H. O. Sorensen, "Quantitative comparison of solid-state microwave detectors," *IEEE Trans. Microwave Theory Tech.*, vol. MTT-14, pp. 588–602, Dec. 1966.
[14] I. S. Gradshteyn and I. W. Ryzhik, *Tables of Integrals Series and Products*. New York: Academic Press, 1965.
[15] M. A. Stuchly, A. Kraszewski, and S. S. Stuchly, "Implantable electric field probes—Some performance characteristics," submitted for publication.
[16] E. B. Larsen and F. X. Ries, "Design and calibration of the NBS isotropic electric-field monitor (EFM-5), 0.2 to 1000 MHz," Nat. Bur. Stand. Tech. Note 1033, Mar. 1981.

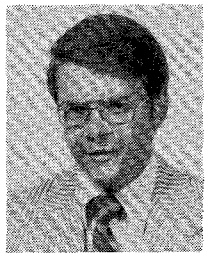

Glenn S. Smith (S'65–M'72) was born in Salem, MA, on June 1, 1945. He received the B.S.E.E. degree from Tufts University, Medford, MA, in 1967 and the S.M. and Ph.D. degrees in applied physics from Harvard University, Cambridge, MA, in 1968 and 1972, respectively.

From 1969 to 1972, he was Teaching Fellow and Research Assistant in Applied Physics at Harvard University. From 1972 to 1975, he served as a Postdoctoral Research Fellow at Harvard University and also a part-time Research Associate and Instructor at Northeastern University, Boston, MA. He is presently as Assistant Professor of Electrical Engineering at Georgia Institute of Technology, Atlanta, GA.

Dr. Smith is a member of Tau Beta Pi, Eta Kappa Nu, and Sigma Xi.

Calculation of TM_{0n} Dispersion Relations in a Corrugated Cylindrical Waveguide

ALAN BROMBORSKY, MEMBER, IEEE, AND BRIAN RUTH

Abstract—**The TM_{0n}-mode Maxwell equations in a cylindrical geometry are converted to a state-vector system of coupled linear differential equations, in which the boundary conditions for a waveguide of varying diameter are included in the coefficient matrix of the state-vector system. The particular problem of periodic boundary conditions is solved for a waveguide with a sinusoidally undulating wall.**

I. Introduction

THE GENERATION of ultra-high-power ($\sim$1 GW) microwave pulses, via the driving of slow-wave structures by intense, pulsed, relativistic electron beams (0.5 to 2.0 MeV, 2 to 15 kA, 15 to 100 ns) [1], [2], places unique demands upon the slow-wave structure in terms of the RF power densities (0.3 GW/cm^2) and electric fields (400 kV/cm) present in the structure. Conventional slow-wave structures, such as the helix- and iris-loaded waveguides, are susceptible to high-field breakdown, and hence plasma formation, with the subsequent shorting out of the slow-wave structure. What is required for ultra-high-power devices is a structure with a periodic wall shape that does not lead to undue electric-field intensification. A possible candidate is a cylindrical guide in which the waveguide diameter varies sinusoidally with axial position.

However, in order to design a device utilizing such a structure, the cold waveguide dispersion relation and the electromagnetic field distribution must be accurately determined.

The basic objective of this paper is to describe a technique for computing the dispersion relation and electromagnetic fields of the TM_{0n} modes of a periodically rippled cylindrical waveguide. Please note that the technique to be described also can be applied to other than TM_{0n} modes, so that with minor changes the derivation could be quite useful in calculating TE modes in tapered gyrotron cavities. Also note that the source terms in the Maxwell equations are not initially set to zero. This is done so that eventually the field calculation described can be used to compute the coupling impedance between an electron beam and a propagating waveguide mode.

Manuscript received August 31, 1983; revised February 6, 1984.
The authors are with the Department of the Army, Harry Diamond Laboratories, Adelphi, MD 20783.

II. Scaling of Maxwell Equations

A. Notation

We define (in MKS units)

c	free-space speed of light,
ϵ_0	permittivity of free space,
μ_0	permeability of free space,
η_0	free-space wave impedance (377 Ω),
ω	wave circular frequency,
r, θ, z	cylindrical coordinates,
E_r, E_θ, E_z	electric-field components,
H_r, H_θ, E_z	magnetic-field components,
J_r, J_θ, J_z	current-density components,
L	periodicity length of slow-wave structure,

0018-9480/84/0600-0600$01.00 ©1984 IEEE